A mathematical model for the first derivative wave analysis of the volumetric capnogram from the perspective of erythrocyte motion profiles

Kyongyob Min [a,*], Shinichi Wada [b]

[a] Respiratory Division of Internal Medicine, Itami City Hospital, Japan
[b] Department of Medical Technology, Faculty of Health Sciences, Kagawa Prefectural University of Health Sciences, Japan

ARTICLE INFO

ABSTRACT

Current trends in monitoring system are leading to the adoption of volumetric capnogram (Vcap). The first derivative wave analysis (FDWA) of Vcap represented the cardiogenic oscillations (CarO) as a propagated wave and the slope of phase III (S_{III}) as a constant. Until today the genesis of CarO and S_{III} is however under debate. In this study, we defined motion profiles of erythrocytes in the pulmonary parenchyma as pulsated-run and random-walk, on the basis of which we obtained a new mathematical expression describing FDWA of Vcap. The mathematical model of Vcap provided theoretical explanation concerned with motion profiles of erythrocytes about the genesis of CarO and S_{III}. As the results, the mathematical model predicted the close relationship between S_{III} and the transfer factor of carbon monoxide, which will be used for estimating validity of this mathematical model. In addition, the velocity of propagated wave in the phase III was suggested as a new physiological variable to estimate elastic properties of pulmonary arterioles, and a new measuring method of V_D was proposed based on the theoretical reason, as well. Clinical investigations of the new V_D to test its efficacy of monitoring are needed.

1. Introduction

Carbon dioxide concentration can be plotted against expired volume (volumetric capnogram, Vcap) during the respiratory cycle. The current trends in monitoring patient safety are leading to the adoption of the capnogram as a standard of care in intensive care units and the importance of Vcap has been recognized (Walsh et al., 2011). One of the earliest descriptions of Vcap and a method to determine "airway" dead space is that of Aitken and Clark-Kennedy (1928). Fowler (1948) in describing the single breath test for nitrogen ($SBT-N_2$) curve sought to use uniform terminology to clarify the "meaning of dead space", and divided this curve into four phases (I, II, III, and IV). Vcap of single breath test ($SBT-CO_2$) also represents four phases resembling $SBT-N_2$ in shape (Bartels et al., 1954). The phase III of Vcap indicates "physiological or alveolar dead space", which means lung units that are ventilating but not contributing to gas-exchange because of no contact with pulmonary capillary blood flow.

"Cardiogenic oscillation" (CarO) is seen in phase III of $SBT-N_2$. CarO has been usually explained by heart beat pulsation transmitted to the lung parenchyma, which represents that resulting changes in the lung volume are sufficient to move small amounts of gas back and forth. However, another explanation for CarO has also been proposed as cyclic

changes in pulmonary arterial pressure and flow (Tusman et al., 2009; Suarez-Sipmann et al., 2013). A recent study of Wada et al. (2015, Fig. 1A) has proposed a new graphical analysis of $SBT-N_2$ (named as "the first derivative wave analysis of $SBT-N_2$" or $FDWA-N_2$) by use of the central difference method (Davis and Polonsky, 1972) of digital data, and has revealed that CarO is seen in both III and IV phases of $FDWA-N_2$, and that the phase III is discriminated from the phase IV by difference in amplitudes of CarO, as well. CarO is important to identify the phase III but its genesis is under debate even today.

The lungs are the primary organs of gas exchange. Gas exchange of oxygen (O_2) and carbon dioxide (CO_2) molecules is a physiological process through which different gas molecules are transferred in opposite directions across a specialized respiratory surface. Classical physiology explains this process in the lung as a result of physical diffusion down a concentration gradient: gas molecules moving from an area of high concentration to low concentration (Wagner, 2005). Classical physiology also explains that both O_2 and CO_2 are transported throughout the body in erythrocytes through arteries, capillaries and veins. O_2 molecules bind to hemoglobin in erythrocytes, and CO_2 molecules dissolve in the plasma or combine with water to form bicarbonate ions (HCO_3^-) with catalyzing action of the carbonic anhydrase (CA) in the erythrocytes. It is well

---

* Corresponding author.
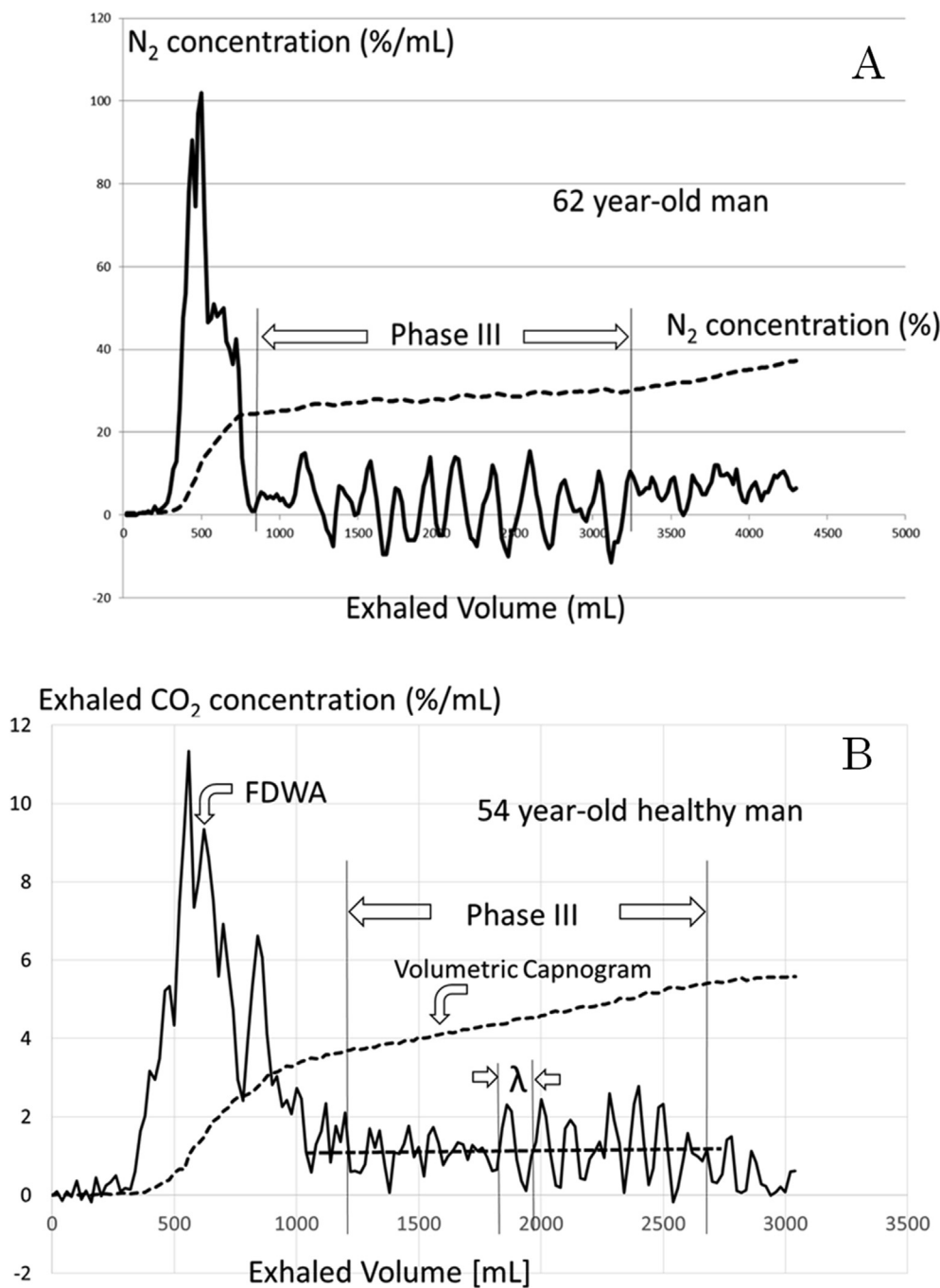*E-mail address:* in1007@osaka-med.ac.jp (K. Min).

Fig. 1. First Derivative Wave Analysis (FDWA) for a single breath test (SBT) for nitrogen (N_2) and for carbon dioxide (CO_2). A: A sample of FDWA-N_2 from Wada et al. (2015); Both usual drawing graph of SBT-N_2 (the dot line) and corresponding FDWA-N_2 graph (solid line) of 62-year old healthy man are shown. Note that cardiogenic oscillations (CarO) were seen in phases III and IV by FDWA-N_2. B: Both a SBT-CO_2 curve (dot line) of a 54-year-old healthy male and its corresponding FDWA-CO_2 (solid line) was displayed in Fig. 2B; note that FDWA is composed of the oscillated part and the constant one in the phase III, and the wave length of cardiogenic oscillation is measured as λ from CarO of the latter part of phase III.

known that erythrocytes play the major role of exchanging gas molecules in the lung. (Klocke, 1997) Recent progress in imaging techniques has provided direct observations on oxygenation process of each erythrocyte in the pulmonary parenchyma including arterioles and capillaries, which showed that each erythrocyte performs gas-exchange while moving in the arterioles and capillaries (Tabuchi et al., 2013).

The lung parenchyma is composed of the secondary pulmonary lobules of Miller or the pulmonary lobule of Matsumoto (Miller, 1937; Matsumoto, 1977). The pulmonary lobule is known as a fundamental unit of lung that can reproduce as a miniature the lung structure (Webb, 2006), where pulmonary airways, arteries, veins, lymphatics and the lung interstitium are represented all at its level. That is, the lung parenchyma is composed of aggregated pulmonary lobules, each of which contains arterioles, venules and alveolar capillary beds where

erythrocytes perform gas exchange. Therefore, if gas-exchange occurs along arterioles/venules and capillary in the pulmonary lobule, the pulmonary lobule should be described as the functional unit of gas-exchange.

In this paper, the authors defined the pulmonary lobule as the functional unit of gas-exchange, and motion profiles of erythrocytes either as percolation along random-walk in the capillaries or as pulsated-run in the arterioles and venules of the pulmonary lobule. Based on different behaviors of erythrocytes during gas exchanging, we obtained a new mathematical expression for Vcap in the form of FDWA-CO_2, which revealed that CarO and the phase III respectively would come from different motion profiles of erythrocytes in the pulmonary parenchyma. By use of the mathematical expression of Vcap, we proposed a new theoretical evaluation method of the dead space.

2. Model

2.1. Physiological and anatomical summary as assumptions for modeling

Physiological and anatomical observations of O_2–CO_2 exchange were summarized as follows (Klocke, 1997; Tabuchi et al., 2013, and Matsumoto, 1977), (A1) the erythrocyte produces carbon dioxide molecules from bicarbonate ions in the plasma by a constant rate; (A2) the erythrocyte captures oxygen molecules from the alveolar space by changing the oxygen affinity of hemoglobin molecules (Hb) according to the oxygen equilibrium curve (OEC), which is considered as a statistical curve in number of saturated erythrocytes among a vast number of erythrocytes in the same condition of oxygen pressure; (A3) oxygenation of erythrocytes occurs within 100 msec over a distance of approximately 10 μm in the pulmonary microvasculature, and approximately 50% of oxygenation occurs in pre-capillary arterioles and post-capillary venules; (A4) in the pulmonary secondary lobule, CO_2 production and O_2 uptake are carried out in erythrocytes moving in the precapillary arterioles, the postcapillary venules, and the capillary beds; (A5) the plot of blood flow velocities (Tabuchi et al., 2013) demonstrated the velocity profile of relatively high blood flow velocities in both the arteriole and the venule segments, and of almost zero flow velocities in the alveolar capillary beds, in other words the former is called pulsated-run and the latter is called random-walk; and (A6) a geometrical analysis of precapillary arterioles has revealed that precapillary arterioles ("spider's pedate arterioles" named by Matsumoto, 1977) are all almost same in the diameter and the length in the secondary pulmonary lobule, and precapillary arterioles and postcapillary venules were not able to be discriminated by their anatomical structures. Weibel (1963) characterized the structural geometry of alveolar capillaries as a two-dimensional stochastic network of short cylindrical tubes with the average form of hexagonal wedges. However, in this study we adopted a lattice form of network consisting of equal length of short cylindrical tubes.

2.2. Random-walk model of erythrocytes in the capillary beds

A random-walk model of gas-exchange at erythrocytes moving in the capillary beds was constructed as follows, (1) as an erythrocyte travels across capillary networks in the alveolar surface, the path traced by the erythrocyte consists of a succession of random steps; (2) the alveolar capillary bed is a large two-dimensional square lattice of sites with the distance θ between them, where each edge is independently opened (allowing the erythrocyte to go through it) with probability p or closed (preventing the erythrocyte from going through it) with probability (1 - p); (3) consider a trajectory as a cluster of connected neighboring sites along random-walk of an erythrocyte.

According to the assumption (A1), each erythrocyte can produce the number of CO_2 molecules (J_{CO_2}) proportional to the number of random steps (s) of its corresponding trajectory as follows,

$$J_{CO_2} \propto s \tag{E1}$$

Based on the assumptions (A2) and (A3), each erythrocyte can capture O_2 molecules (J_{O_2}) by changing the oxygen-saturation of Hb (ΔS_{O_2}) during more steps than the critical number of steps, s_m,

$$J_{O_2} \propto \Delta S_{O_2} \cdot \delta_{s,s_m} \tag{E2}$$

where δ_{s,s_m} is a step function ($\delta_{s,s_m} = 0$, if $s < s_m$; $\delta_{s,s_m} = 1$, if $s \geq s_m$).

3. Results

3.1. Random-walk and a diffusion equation

A trajectory of random walk from zero to step s has to obey the master equation as follows (Stauffer and Aharony, 1994),

$$P_i(s+1) - P_i(s) = \sum_j \left[\sigma_{ji} P_j(s) - \sigma_{ij} P_i(s) \right] \tag{E3}$$

where $P_i(s)$ is the probability occupied at the site i by an erythrocyte at the step s, and σ_{ij} is the probability of transition from the site i to its adjacent site j with the probability of p during between steps s and $s+1$. The alveolar capillary network is defined as a square lattice (x,y) of distance θ between adjacent sites, where erythrocytes move randomly with a probability p during the time t and $t + \varepsilon$. Since the alveolar capillary network is a square lattice, the transitional probability σ_{ij} is $p/4$. At the time $t + \varepsilon$, the probability of finding the erythrocyte at the site (x, y) is described as follows,

$$P(x, y, t + \varepsilon)$$

$$= \frac{p}{4} \{ P(x + \theta, y, t) + P(x - \theta, y, t) + P(x, y + \theta, t) + P(x, y - \theta, t) \} \tag{E4}$$

Then, the subtraction $P(x, y, t + \varepsilon) - p(x, y, t)$ is expressed as follows,

$$P(x, y, t + \varepsilon) - P(x, y, t)$$

$$= \frac{p}{4} \{ P(x + \theta, y, t) - 2P(x, y, t) + P(x - \theta, y, t) + P(x, y + \theta, t)$$
$$+ P(x, y - \theta, t) - 2P(x, y, t) \} \tag{E5}$$

A set of approximations are known as follows,

$$P(x + \theta, y, t) - 2P(x, y, t) + P(x - \theta, y, t) \sim \frac{\partial^2 P}{\partial x^2} \theta^2 \tag{E6}$$

$$P(x, y + \theta, t) - 2P(x, y, t) + P(x, y - \theta, t) \sim \frac{\partial^2 P}{\partial y^2} \theta^2 \tag{E7}$$

Therefore, the Eq. (E8) is obtained by $\varepsilon \to 0$ from the Eq. (E5) as follows,

$$\frac{\partial P}{\partial t} = \left(\frac{p\theta^2}{4} \right) \left(\frac{\partial^2 P}{\partial x^2} + \frac{\partial^2 P}{\partial y^2} \right) \tag{E8}$$

$$D_{rw} = \frac{p\theta^2}{4} \tag{E9}$$

The Eq. (E8) has represented a two-dimensional diffusion phenomenon of the diffusion coefficient D_{rw}, which contains a physiological parameter p and a geometrical parameter $\theta^2/4$.

3.2. Percolation (Fig. 2A, B)

It is necessary for every erythrocyte to pass through the capillary beds from the arteriole side to the venule side (percolation) in order to do effective gas exchange. Percolation theory describes trajectories of erythrocytes according to the master Eq. (E3), and can answer the question, "what is the probability that erythrocytes can pass from arterioles to venules under a given opening probability of p?" Computer simulations (Sedgewick and Wayne, 2016, Fig. 2B) have shown that the probability of a connected path from the arteriole side to the venule side increases sharply from close to 0 to close to 1 within a short span of p. Therefore, there is a critical probability (p_c): the percolation probability is 0 or 1 at less and more than it, respectively. That is, when the opening probability p of capillary branch is more than p_c, every erythrocyte can reach corresponding postcapillary venules. As suggested in the experimental study by Presson and colleagues (Presson et al., 1997) the opening probability p of capillary branch would be dependent upon the microvascular pressure of alveolar capillaries. If the capillary pressure is less than the critical value, oxygen-saturated erythrocytes cannot reach corresponding venules and cannot contribute to oxygenation of total blood. However, CO_2 shift from blood into alveolar spaces must be independent from percolation process of erythrocytes because erythrocytes
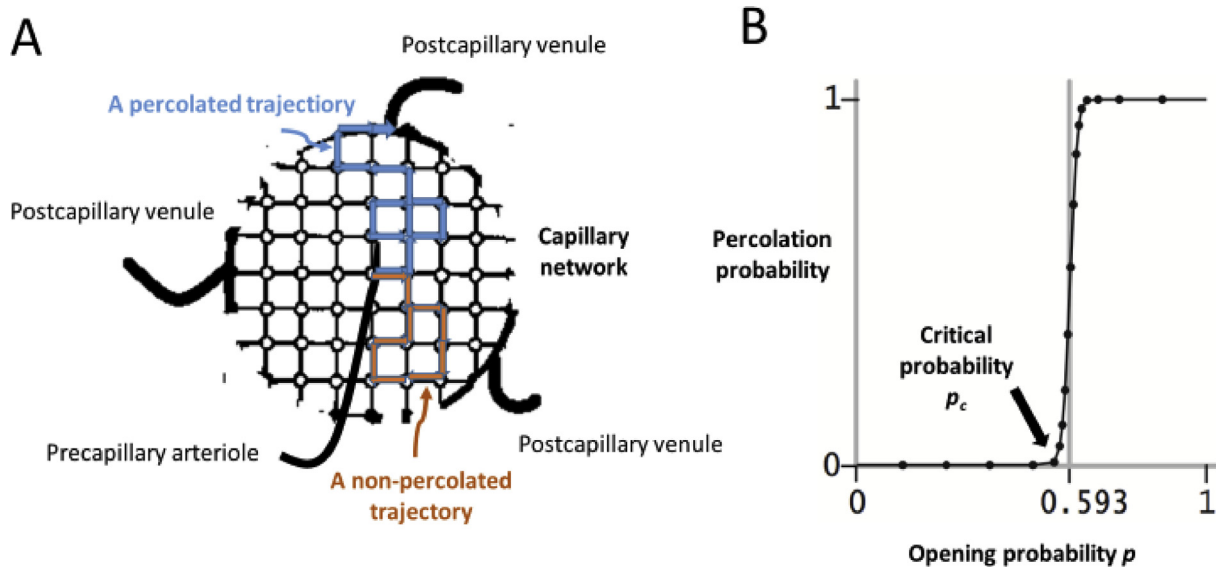
Fig. 2. Capillary Network and Percolation. A: A large number of erythrocytes come in the capillary beds by pulsated-runs through the precapillary arterioles, and are distributed in capillary beds by random walks. Two types of trajectory of each erythrocyte by random-walk are presented; the first (blue) trajectory is a path from an arteriole to a venule, another (red) is a path of sustained stay in the capillary bed. B: A sample of Monte Carlo simulation by Sedgewick and Wayne (2016), who showed the site vacancy probability p versus the percolation probability for 100-by-100 random grid with a Java programming environment. This graph indicates that pulmonary capillary perfusion would appear by all-or-none style, which was reported by Presson et al. (1997).

in the pulmonary parenchyma produce CO_2 from plasma at constant rate. Thus, percolation of erythrocytes across the capillary beds would make some significant difference between O_2-uptake and CO_2-elimination in the pulmonary parenchyma.

3.3. Two types of motion profiles

3.3.1. Proportion of motion profiles in the transit time

Erythrocytes are running in the pulmonary parenchyma which consists of the pulmonary secondary lobule of Miller. Based on the assumption (A6) the pulmonary secondary lobule contains intralobular arterioles, alveolar capillary beds and intralobular venules, and according to the assumption (A5) two types of motion (pulsated-run in the arterioles/venules and random-walk in the capillary beds) would be seen in the pulmonary parenchyma. No precise description about the proportion of number of erythrocytes in either pulsated-run or random-walk has been reported until today.

Transit time (τ) for each erythrocyte passing through the pulmonary parenchyma is composed of both the time in pulsated-run (τ_{pul}) and that in random-walk (τ_{rw}); i.e., $\tau = \tau_{pul} + \tau_{rw}$. When the ratio of τ_{rw} and τ is described by μ, each transit time is defined as follows,

$$\tau_{pul} = (1 - \mu)\,\tau \tag{E10}$$

$$\tau_{rw} = \mu\,\tau \tag{E11}$$

3.3.2. Gas-exchange in an erythrocyte

Gas exchange is performed by each erythrocyte during both motion profiles of pulsated-run and of random-walk. If the transit time is proportional to the number of steps, each erythrocyte can produce the number of CO_2 molecules (J_{CO_2}) that is proportional to its transit time (τ) in the pulmonary lobule as follows,

$$J_{CO_2} \propto \tau = \left(\tau_{pul} + \tau_{rw}\right) = \tau(1 - \mu) + \tau(\mu) \tag{E12}$$

Each erythrocyte can capture O_2 molecules by changing the oxygen-saturation of Hb molecules themselves (ΔS_{O_2}) during the passing across the pulmonary lobule according to (E2). Since the time of pulsated-run (τ_{pul}) would usually be longer than the sufficient time (τ_m) necessary

for complete saturation of Hb, from (E2) the equation for capturing oxygen molecules by an erythrocyte was defined as follows,

$$J_{O_2} \propto \Delta S_{O_2}\delta_{\tau,\tau_m} = \Delta S_{O_2}\left(\delta_{\tau_{pul},\tau_m} + \delta_{\tau_{rw},\tau_m}\right)/2 = \Delta S_{O_2}(1 + f_{rw})/2 \ldots \tag{E13}$$

where $\delta_{\tau_{pul},\,\tau_m}$ or $\delta_{\tau_{rw},\,\tau_m}$ is the step function ($\delta_{\tau,\,\tau_m} = 0$ if $\tau < \tau_m$, $\delta_{\tau,\,\tau_m} = 1$ if $\tau \geq \tau_m$), respectively, and f_{rw} is the fractional ratio of erythrocytes passed longer than the critical time (i.e., $f_{rw} = \sum_{\tau_{rw}}\delta_{\tau_{rw},\tau_m}/N_e$, where N_e is the total number of erythrocytes passed through capillary beds).

3.3.3. Gas-exchange equations and Vcap

According to the classical physiology of pulmonary gas-exchange equations, a set of equations for gas-exchange in the pulmonary lobule of l is expressed as follows (Wagner, 2005),

$$P^l_{ACO_2} \cdot V^l_A \propto (C_{vCO_2} - C_{aCO_2}) \cdot q^l \tag{E14}$$

$$P^l_{AO_2} \cdot V^l_A \propto (C_{aO_2} - C_{vO_2}) \cdot q^l \tag{E15}$$

where $P^l_{ACO_2}$ and $P^l_{AO_2}$ are the alveolar carbon dioxide pressure and the alveolar oxygen pressure in the pulmonary lobule l, respectively; V^l_A is the alveolar ventilation volume of the pulmonary lobule l; C_{vCO_2}, C_{vO_2}, C_{aCO_2}, and C_{aO_2} are contents of carbon dioxide and oxygen gases in the pulmonary venous and arterial blood, respectively; and q^l is the blood flow including a number of erythrocytes n^l_e into the pulmonary secondary lobule of l. When the average of transit times among erythrocytes in the pulmonary lobule l is $\overline{\tau}^l(= \overline{\tau}^l_{pul} + \overline{\tau}^l_{rw})$, from Eqs. (E14) and (E15) a new set of equations for the lobular gas-exchange is obtained as follows,

$$P^l_{ACO_2} \cdot V^l_A \propto (C_{vCO_2} - C_{aCO_2}) \cdot q^l \propto n^l_e \cdot \overline{\tau}^l = n^l_e\left(\overline{\tau}^l_{pul} + \overline{\tau}^l_{rw}\right) = n^l_e\overline{\tau}^l_{pul} + n^l_e\overline{\tau}^l_{rw}$$
$$= N^l_e\left(1 - \mu^l\right) + N^l_e\mu^l \tag{E16}$$

$$P^l_{AO_2} \cdot V^l_A \propto (C_{aO_2} - C_{vO_2}) \cdot q^l \propto n^l_e \cdot \overline{\tau}^l \cdot \Delta S^l_{O_2}\left(1 + f^l_{rw}\right)/2 \propto N^l_e\left(1 - \mu^l\right) \cdot S^l_{O_2}$$
$$+ N^l_e\mu^l \cdot S^l_{O_2}f^l_{rw} \tag{E17}$$

where suffix l indicates that every parameter is observed in the lobule l, and N_e^l is total number of erythrocytes in the lobule l. When N number of lobules are contributing to a volume of ventilate V_A, the equation of gas-exchange (P_{ACO_2} and P_{AO_2}) for the lung can be obtained by summation of (E16) or (E17) through the whole lung as follows,

$$P_{ACO_2} \cdot V_A = \sum_{l=1}^{N} P_{ACO_2}^l \cdot V_A^l \propto \sum_{l=1}^{N} \left\{ N_e^l \left(1 - \mu^l \right) + N_e^l \mu^l \right\}$$

$$= N_e(1 - \mu) + N_e\mu \qquad (E18)$$

$$P_{AO_2} \cdot V_A = \sum_{l=1}^{N} P_{AO_2}^l \cdot V_A^l \propto \sum_{l=1}^{N} \left\{ N_e^l \left(1 - \mu^l \right) \Delta S_{O_2}^l + N_e^l \mu^l \Delta S_{O_2}^l f_{rw}^l \right\}$$

$$= \Delta \overline{S}_{O_2}(1 - \mu)N_e + \Delta \overline{S}_{O_2} \mu N_e \overline{f}_{rw} \qquad (E19)$$

where N_e is the total number of erythrocytes, and $\Delta \overline{S}_{O_2}$, $\overline{f}_{rw}$, or μ is the mean value of $\Delta S_{O_2}^l$, f_{rw}^l, or μ^l respectively among pulmonary lobules contributing to the exhaled volume of V_A. According to the ergodic rule of statistical physics, it is assumed that the time proportion between motion profiles (μ) would become equal to a topographical proportion between the arterioles/venules and the capillary beds. Therefore, among the total number (N_e) of erythrocytes contributing to the exhaled volume of V_A, the number of erythrocytes in pulsated run was defined by $N_e(1 - \mu)$, and those in random walk was defined by $N_e\mu$.

By partial differentiation the Eq. (E18) twice regarding with V_A, we obtained the expression of Vcap as follows,

$$\frac{\partial P_{ACO_2}}{\partial V_A} \propto (1 - \mu) \frac{\partial^2 N_e}{\partial V_A^2} + (\mu) \frac{\partial^2 N_e}{\partial V_A^2} \qquad (E20)$$

Concerning the type of motion profiles for pulsated-run or random-walk, two motion equations were introduced as follows,

$$c^2 \frac{\partial^2 N_e}{\partial V_A^2} = \frac{\partial^2 N_e}{\partial t^2} \quad \text{(the wave equation for pulsated − run)} \qquad (E21)$$

$$D_{rw} \frac{\partial^2 N_e}{\partial V_A^2} = \frac{\partial N_e}{\partial t} \quad \text{(the diffusion equation for random − walk)} \qquad (E22)$$

where c or D_{rw} is respectively a velocity of oscillation-wave or a diffusion coefficient along the axis of V_A. Therefore, Vcap was defined by the motion equation as follows,

$$\frac{\partial P_{ACO_2}}{\partial V_A} \propto \frac{(1 - \mu)}{c^2} \frac{\partial^2 N_e}{\partial t^2} + \frac{\mu}{D_{rw}} \frac{\partial N_e}{\partial t} \qquad (E23)$$

3.3.4. First derivative wave analysis of Vcap

Pulmonary blood flow is produced by both cardiac contraction and elastic pulmonary arterial wall. Erythrocytes run through pulmonary parenchyma along with pulmonary blood flow. Right heart catheterization has revealed that pulmonary arterial blood flow is composed of the oscillated part and the constant part. Thus, the total number of erythrocytes (N_e) in the pulmonary blood flow would be expressed as follows,

$$N_e(t) = \int_0^t Ag(u)du + Bt \qquad (E24)$$

where $Ag(t)$ and B are respectively the oscillated part and the constant part. Thus, the equation for Vcap was expressed as follows,

$$\frac{\partial P_{ACO_2}}{\partial V_A} \propto \frac{(1 - \mu)}{c^2} \frac{\partial^2 N_e}{\partial t^2} + \frac{\mu}{D_{rw}} \frac{\partial N_e}{\partial t}$$

$$= \left[\frac{(1 - \mu)}{c^2} \frac{\partial}{\partial t} + \frac{\mu}{D_{rw}} \right] Ag(t) + \left(\frac{\mu}{D_{rw}} B \right) \qquad (E25)$$

(E25) has showed that Vcap consists of the oscillating part and the constant part; the first clause represents the forced oscillating system of the damper $(1 - \mu)/c^2$ driven by the periodic force of $Ag(t)$ ("cardiogenic oscillation"), and the second clause represents that the gradient of phase III comes from random-walk of erythrocytes in the capillary beds.

3.3.5. Transfer factor of CO diffusion (T_{co}) and slope of phase III

The rate of carbon monoxide (CO) uptake from the lungs is the product of alveolar partial pressure of CO in excess of any back pressure in the blood (driving pressure) and a rate constant. The single breath diffusing capacity method is performed by having the subject blow out as much air as possible, leaving only the residual lung volume. The subject then rapidly and completely inhales a gas mixture containing a tracer gas such as helium, reaching the total lung capacity as much as possible. The tracer gas is held in the lung for about 10 seconds during which time the CO continuously moves from pulmonary parenchyma into the blood. The CO uptake from the lung (D_{LCO}) is measured as a change in concentration of CO per a change in pressure. Since molecules of CO have very high affinity to hemoglobin molecules (Hb), Hb in each erythrocyte in the alveolar capillary beds would be rapidly and completely saturated ($\Delta \overline{S}_{CO} = 1.0$) during the time of Δt. Thus, $\overline{f}_{rw}$ and $\Delta \overline{S}_{CO}$ respectively must be 1.0 in (E19). The equation for CO uptake in the single breath diffusion capacity method is described by the same equation as (E20) as follows,

$$\frac{\partial P_{ACO}}{\partial V_A} \propto \left[\frac{(1 - \mu)}{c^2} \frac{\partial}{\partial t} + \frac{\mu}{D_{rw}} \right] Ag(t) + \left(\frac{\mu}{D_{rw}} B \right) \qquad (E26)$$

Then, the transfer factor for CO ($T_{CO} = D_{LCO}/V_A$) would be proportional to the slope of phase III of Vcap as follows,

$$T_{CO} = \int_0^{10} \frac{dP_{ACO}}{dV_A} dt \propto \int_0^{10} \left[\frac{(1 - \mu)}{c^2} \frac{\partial}{\partial t} + \frac{\mu}{D_{rw}} \right] Ag(t) dt$$

$$+ \int_0^{10} \left(\frac{\mu}{D_{rw}} B \right) dt \propto \left(\frac{\mu}{D_{rw}} B \right) \qquad (E27)$$

3.3.6. Dead space

The excreted volume of carbon dioxide (E_{ACO_2}) into the pulmonary parenchyma during a tidal breathing of volume V_T or a breath time of T is defined by use of (E25) as follows,

$$E_{ACO_2} = \int_0^{V_T} \frac{dP_{ACO_2}}{dV_A} dV \propto \int_0^{T} \left[\left[\frac{(1 - \mu)}{c^2} \frac{d}{dt} + \frac{\mu}{D_{rw}} \right] Ag(t) + \left(\frac{\mu}{D_{rw}} B \right) \right] dt$$

$$= \left(\frac{\mu}{D_{rw}} B \right) T \qquad (E28)$$

Since the flow rate of carbon dioxide (E_{ACO_2}/T) is proportional to the slope of phase III, E_{ACO_2} during a breath is evaluable as the area of trapezoid 1-2-3-4 (see Fig. 3). The actual excreted volume of CO_2 is measurable as the area under curve of Vcap (AUV_{cap}). Therefore, the dead space in this case must be described by $(1 - AUV_{cap}/E_{ACO_2})V_T$.

4. Discussion

4.1. Geometrical properties of pulmonary capillary network and percolation

Although Weibel (1963) characterized the structural geometry of alveolar capillaries as a two-dimensional stochastic network of short cylindrical tubes with the average form of hexagonal wedges with two adjacent segments, in this study we adopted a lattice form of network consisting of equal length of short cylindrical tubes. Geometrical difference in the capillary network is well known to produce the difference of the critical probability in the percolation phenomenon (p_c in the section

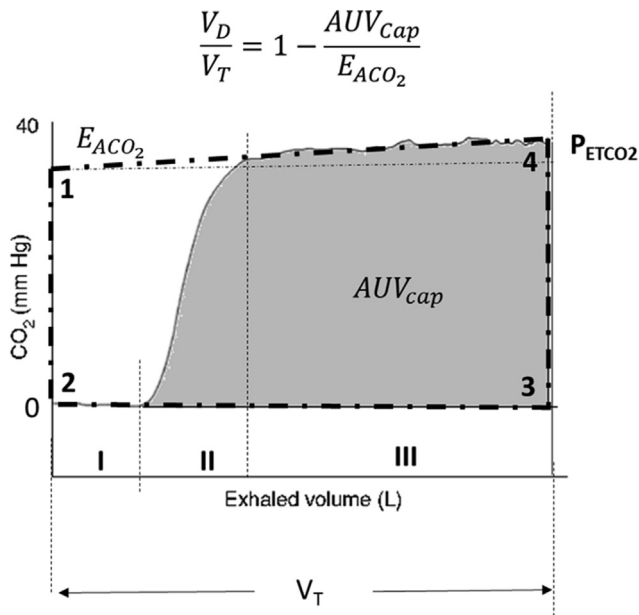$$\frac{V_D}{V_T} = 1 - \frac{AUV_{Cap}}{E_{ACO_2}}$$

Fig. 3. Dead Space. Carbon dioxide from erythrocytes is excreted into the alveoli constantly in the lung parenchyma during a breath. Since the flow rate of carbon dioxide (E_{ACO_2}/T) is proportional to the slope of phase III, E_{ACO_2} during a breath is evaluable as the area of trapezoid 1-2-3-4. The area under Vcap ($AUVcap$) is the total volume of exhaled CO_2 from the pulmonary parenchyma during a breath. The dead space normalized by tidal volume (V_T) is expressed by the ratio $(1 - AUV_{cap}/E_{ACO_2})$.

3.2, $p_c = 0.6962$ for honeycomb and $p_c = 0.592746$ for square). (Broadbent and Hammersley, 2008) However, it is noted that motion profiles of erythrocytes are described by the diffusion equation of a corresponding appropriate diffusion coefficient even in different forms of network like the equation of (E8). Anyway, it is important to recognize that pulmonary perfusion is achieved by the rule of all-or-none based on percolation theory.

4.2. CarO and phase III in FDWA-CO$_2$

4.2.1. The first derivative wave analysis (FDWA)

By constructing the ratio of a change in N$_2$ concentration of exhaled gas with regard to the change of exhaled lung volume (20ml), Wada and colleagues (Wada et al., 2015) introduced a new graphical analysis of SBT-N$_2$ curve (FDWA-N$_2$, Fig. 1A) where the phase III was composed of cardiogenic oscillations (CarO) and constant (which indicates the slope of phase III in SBT-N$_2$). It was able to distinguish phase IV from phase III using the difference in amplitude of CarO in FDWA-N$_2$. In this study we applied FDWA to the volumetric capnogram of single breath test (SBT-CO$_2$). CarO have been neglected in usual SBT-CO$_2$ because of being less than SBT-N$_2$. FDWA-CO$_2$ showed however clear oscillations in the latter part of phase III as shown in Fig. 1B, which is composed of noisy changes of small amplitude in the early part followed by large amplitudes of waves. CarO of FDWA-CO$_2$ would be explained as a resonance in forced damping oscillations based on the mathematical model of (E25).

The velocity (c) representing the cardiogenic waves in FDWA-CO$_2$ is evaluable by product of λ (the wave length) and ν (the heart rate). Since the parameter c represents pulsated-run in arterioles/venules in the pulmonary parenchyma, the parameter c would become useful for diagnosing pulmonary vascular diseases. For confirming this hypothesis
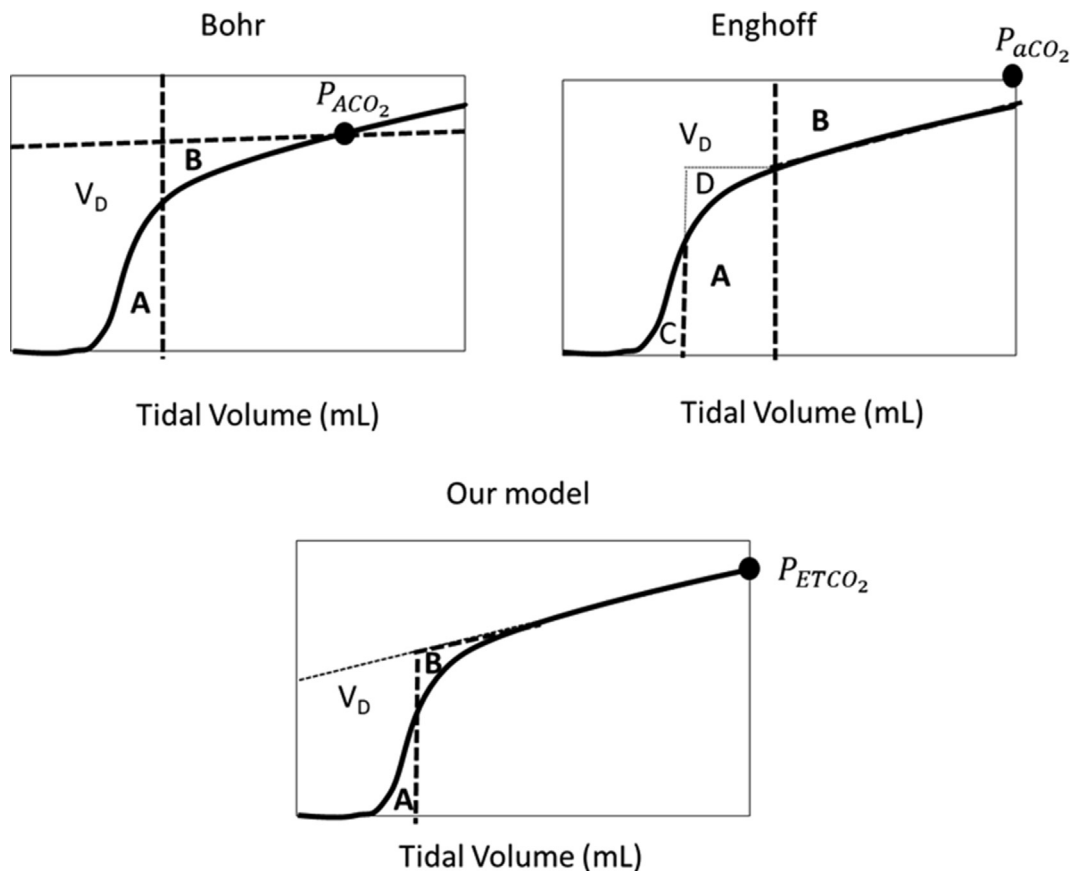

Fig. 4. Difference among Bohr, Enghoff, and our approaches to Dead space. The line discriminating the dead space from the tidal volume is created so that the area A equals to the area B. In the case of Enghoff, the line is created so that the area C equals to the area D. The dead space (V_D) is different among approaches, and V_D of our model seems the smallest.

clinical studies are needed.

4.2.2. Slope of phase III

The origin of phase III slope has been attributed to 1) continuous excretion of N_2 into the alveoli becoming smaller by the end of expiration, and/or 2) late emptying of alveoli with low ventilation-perfusion ratio containing relatively higher N_2 concentration. The standard explanation of phase III slope is based on the concept that gravity causes uneven ventilation in the lung through the deformation of lung tissue (Slinky effect), and uneven perfusion through combination of the Slinky effect and the zone model of pulmonary perfusion. However, when SBT-N_2 were performed repeatedly in parabolic flights and in spaceflights, all of the signatures of ventilator heterogeneity persisted. The terminal rise in N_2 concentration in SBT-N_2 (phase IV) was greatly reduced in microgravity, but the persistence of a phase IV is evidence that both ventilation and perfusion exhibit persisting heterogeneity in microgravity indicating important other mechanisms (Prisk, 2014).

Our mathematical model in this study can provide another gravity independent mechanism for phase III: since the number of erythrocytes µB is a constant flux of erythrocytes flouring into the pulmonary capillary beds, the mathematical expression (E25) has revealed the slope of phase III ($\mu B / D_{rw}$) in Vcap represents the gradient in number of erythrocytes between sides of arterioles and venules in the pulmonary capillary beds. As reported experimental study of Presson et al. (1997), the gradient of erythrocytes in number would relate to microvascular pressure in the capillary beds. Thus, since pulmonary microvascular pressure change in the microgravity environment would be most important to understand the phase III, it is necessary to investigate what physiological and geometrical changes are seen in pulmonary vascular system under the microgravity environment.

T_{CO} of (E27) suggested a close relationship between the phase III slope and T_{CO}, both of which represents the gradient in number of erythrocytes between the pulmonary arterioles and venules. Thus, the validity of our mathematical model would be evaluated by a close relationship between T_{CO} and the phase III slope of Vcap among various conditions including parenchymal lung diseases.

4.3. Dead space

The dead space (V_D) refers to lung units that are ventilated but do not contribute to gas exchange because the expired gas from these units has no contact with pulmonary capillary blood flow. In 1891, Bohr proposed an equation to calculate dead space normalized tidal volume (V_T):

$$V_D / V_T = \left(P_{ACO_2} - P_{\bar{E}CO_2} \right) \Big/ P_{ACO_2}$$

P_{ACO_2} is alveolar P_{CO_2} and $P_{\bar{E}CO_2}$ is mixed expired P_{CO_2}. However, P_{ACO_2} is not readily available. In 1938, Enghoff proposed an adaptation of Bohr's equation in which P_{aCO_2} is used instead of P_{ACO_2}. Substitution of P_{aCO_2} for P_{ACO_2} produces some confusion in the interpretation of the mechanism of dead space production. As the discussion by Verscheure et al. (2016), Enghoff's substitution has been known as valid only in an ideal lung of perfect ventilation-perfusion matching for all units, but is never applicable to the case of pulmonary diseases.

By use of an equal area method proposed by Tang et al. (2006), we have also described difference among Bohr, Enghoff, and our approaches to the dead space in Fig. 4, in which the line discriminating between the dead space (V_D) and the alveolar gas-exchange space is created so that area A equals to area B. Our model would provide the smallest V_D among three models as the real dead space because that CO_2 molecules may distribute diffusely in the pulmonary parenchyma including bronchioles. At the bedside Vcap will allow us more precise measurement of real dead space on a breath-by-breath basis. Therefore, we will propose that further

clinical research on dead space of Vcap measured by our model is necessary for guiding effective therapy in the emergency department, operating room and intensive care unit.

5. Conclusion

On the basis of motion profiles of erythrocytes in the pulmonary parenchyma, a new mathematical expression for the volumetric capnography (Vcap) was proposed in this paper. The mathematical expression of Vcap provided theoretical explanations for genesis of the phase III slope and of cardiogenic oscillations (CaRO), respectively. Validity of our mathematical model will be assessed by the close relationship between the slope of phase III of Vcap and the transfer factor of CO. In addition, the velocity of CaRO in the first derivative wave analysis (FDWA) of Vcap was suggested as a physiological indicator for estimating elastic properties of pulmonary arterioles. We have also proposed a more precise measurement of dead space based on the mathematical model. For guiding more appropriate therapy of patients in the emergency department, operating room and intensive care unit, clinical researches by use of our measurement of dead space are needed.

References

Aitken, R.S., Clark-Kennedy, A.E., 1928. On the fluctuation in the composition of the alveolar air during the respiratory cycle in muscular exercise. J. Physiol. 65, 389–411.

Bartels, J., Severinghaus, J.W., Forster, R.E., Briscoe, W.A., Bates, D.V., 1954. The respiratory dead space measured by single breath analysis of oxygen, carbon dioxide, nitrogen or helium. J. Clin. Investig. 33 (1), 41–48.

Broadbent, S.R., Hammersley, J.M., 2008. Percolation processes. Math. Proc. Camb. Philos. Soc. 53 (03), 629-541.

Davis, P.J., Polansky, I., 1972. Differences. In §25 (Numerical interporation, differentiation and integration). In: Abramowitz, M., Stegun, I.A. (Eds.), Handbook of Mathematical Functions with Formulas, Graphs, and Mathematical Tables, 9th Printing. Dover, New York, pp. 877–878.

Fowler, W.S., 1948. Lung function studies. II. The respiratory dead space. Am. J. Physiol. 154, 405–416.

Klocke, R.A., 1997. In: Crystal, R.G., West, J.B., et al. (Eds.), Carbon Dioxide Transport Chapter 121, THE LUNG: Scientific Foundations, Second ed. Lippincott-Raven, Philadelphia, pp. 1633–1642.

Matsumoto, T., 1977. Lung in Tissue and Organ II, Series of Modern Biological Science. Iwanami Shoten, Tokyo, p. 357 (Japanese).

Miller, W.S., 1937. The Lung. Charles C. Thomas, Springfield, Illinois, USA.

Presson Jr., R.G., Todoran, T.M., De Witt, B.J., McMurtry, I.F., Wagner Jr., W.W., 1997. Capillary recruitment and transit time in the rat lung. J. Appl. Physiol. 83, 543–549.

Prisk, G.K., 2014. Microgravity and respiratory system. Eur. Respir. J. 43, 1459–1471.

Sedgewick, R., Wayne, K., 2016. Case Study: Percolation last modified Aug 02. http://introcs.cs.princeton.edu/java/24percolation/.

Stauffer, D., Aharony, A., 1944. Introduction to Percolation Theory, second ed.

Suarez-Sipmann, F., Santos, A., Peces-Barba, G., Bohm, S.H., Gracia, J.L., Cardero'n, P., Tusman, G., 2013. Pulmonary artery pulsatility is the main cause of cardiogenic oscillations. J. Clin. Monit. Comput. 27 (1), 47–53.

Tang, Y., Turner, M.J., Baker, A.B., 2006. A new equal area method to calculate and represent physiological, anatomical, and alveolar dead spaces. Anesthesiology 104, 696–700.

Tabuchi, A., Styp-Rekowska, B., Slutsky, A.S., Wagner, P.D., Pries, A.R., Kuebler, W.M., 2013. Precapillary oxygenation contributes relevantly to gas exchange in the intact lung. Am. J. Respir. Crit. Care Med. 188, 474–481.

Tusman, G., Suzrez-Sipmann, F., Peces-Barba, G., Climente, C., Areta, M., Arenas, P.G., Bohm, S.H., 2009. Pulmonary blood flow generates cardiogenic oscillations. Respir. Physiol. Neurobiol. 167 (3), 247–254.

Verscheure, S., Massion, P.B., Vershuren, F., Damas, P., Magder, S., 2016. Volumetric capnography: lessons from the past and current clinical applications. Crit. Care 20, p184–192.

Wada, S., Imai, T., Min, K.Y., Ogo, K., Miyamoto, T., Okada, Y., Fujioka, S., 2015. A new method of analyzing the closing volume (CV) curve: "N2 first derivative wave analysis method. Rinsho Byori Jpn. J. Clin. Pathol. 63, 1264.

Wagner, P.D., 2005. The physiological basis of pulmonary gas exchange: implications for clinical interpretation of arterial blood gases. Eur. Respir. J. 45, 227–243.

Walsh, B.K., Crotwell, D.N., Restrepo, R.B., 2011. Capnography/capnometry during mechanical ventilation: 2011. Respir. Care 56 (4), 503–509.

Webb, W.R., 2006. Thin-section CT of the secondary pulmonary lobule: anatomy and the image-the 2004 Fleischner lecture. Radiology 239, 322–338.

Weibel, E.R., 1963. Geometry and Dimensions of Alveolar Capillary Network. Chapter VII, Morphometry of Human Lung. Springer-Verlag Berlin Heiderberg, pp. 73–89.